

Micro/Nanotribology and Its Applications

Bharat Bhushan

Ohio Eminent Scholar Professor and Director, Computer Microtribology and Contamination Laboratory, The Ohio State University Columbus, Ohio 43210, U.S.A.

Abstract—Atomic force microscopy/friction force microscopy (AFM/FFM) techniques are increasingly used for tribological studies of engineering surfaces at scales, ranging from atomic and molecular to microscales. These techniques have been used to study surface roughness, adhesion, friction, scratching/wear, indentation, detection of material transfer, and boundary lubrication and for nanofabrication/nanomachining purposes. Micro/nanotribological studies of single-crystal silicon, natural diamond, magnetic media (magnetic tapes and disks) and magnetic heads have been conducted. Commonly measured roughness parameters are found to be scale dependent, requiring the need of scale-independent fractal parameters to characterize surface roughness. Measurements of atomic-scale friction of a freshly-cleaved highly-oriented pyrolytic graphite exhibited the same periodicity as that of corresponding topography. However, the peaks in friction and those in corresponding topography were displaced relative to each other. Variations in atomic-scale friction and the observed displacement has been explained by the variations in interatomic forces in the normal and lateral directions. Local variation in microscale friction is found to correspond to the local slope suggesting that a ratchet mechanism is responsible for this variation. Directionality in the friction is observed on both micro- and macro scales which results from the surface preparation and anisotropy in surface roughness. Microscale friction is generally found to be smaller than the macrofriction as there is less ploughing contribution in microscale measurements. Microscale friction is load dependent and friction values increase with an increase in the normal load approaching to the macrofriction at contact stresses higher than the hardness of the softer material. Wear rate for single-crystal silicon is approximately constant for various loads and test durations. However, for magnetic disks with a multilayered thin-film structure, the wear of the diamond like carbon overcoat is catastrophic. Breakdown of thin films can be detected with AFM. Evolution of the wear has also been studied using AFM. Wear is found to be initiated at nono scratches. AFM has been modified to obtain load-displacement curves and for nanoindentation hardness measurements with depth of indentation as low as 1 nm. Scratching and indentation on nanoscales are the powerful ways to screen for adhesion and resistance to deformation of ultrathin films. Detection of material transfer on a nanoscale is possible with AFM. Boundary lubrication studies and measurement of lubricant-film thickness with a lateral resolution on a nanoscale have been conducted using AFM. Self-assembled monolayers and chemically-bonded lubricant films with a mobile fraction are superior in wear resistance. Finally, AFM has also shown to be useful for nanofabrication/nanomachining. Friction and wear on micro-and nanoscales have been found to be generally smaller compared to that at macroscales. Therefore, micro/nanotribological studies may help define the regimes for ultra-low friction and near zero wear.

1. Introduction

The recent emergence and proliferation of proximal probes, in particular tip-based microscopies (the scanning tunneling microscope and atomic force microscope) has allowed the study of surface topography, adhesion, friction, wear, lubrication and measurement of mechanical properties all on a micro- to nanometer scale, to image lubricant molecules and availability of supercomputers to conduct a-

tomicro-scale simulations has led to development of a new field referred to as Microtribology or Nanotribology [1,2]. This field concerns with experimental and theoretical investigations of processes ranging from atomic and molecular scales to microscale, occurring during adhesion, friction, wear, and thin-film lubrication at sliding surfaces. These studies are needed to develop fundamental understanding of interfacial phenomena on a small scale and to study interfacial phenomena in micro-

and nano structures used in magnetic storage systems, microelectromechanical systems (MEMS) and other industrial applications. Friction and wear of lightly-loaded micro/nano components are highly dependent on the surface interaction (few atomic layers). These structures are generally lubricated with molecularly-thin films. Micro- and nanotribological studies are also valuable in fundamental understanding of interfacial phenomena in macrostructures [3-5] to provide a bridge between science and engineering.

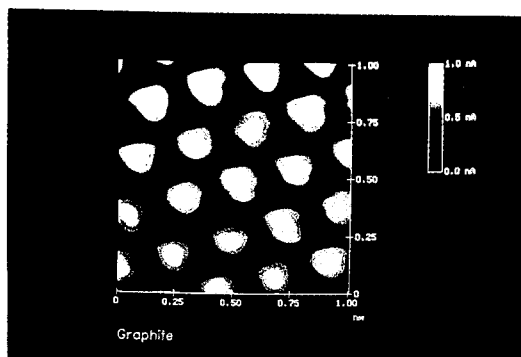
Adhesion [6-10], friction [11-23], wear [15-17,20-22,24] and lubrication [6,25-30] at the interface between two solids with and without liquid films have been studied using the AFM and FFM. At most solid-solid interfaces of technological relevance, contact occurs at numerous asperities [3-5], a sharp AFM/FFM tip sliding on a surface simulates just one such contact. Surface roughness is routinely measured using the AFM [31-34] and it has been used for measuring elastic-plastic mechanical properties [16,17,20-22,35-38]. For measurements of surface roughness, friction force, nanoscale scratching and wear, a microfabricated square-pyramidal Si₃N₄ or silicon tip with a tip radius ranging from 10 to 50 nm is generally used [1] at loads ranging from 10 to 150 nN. For measurements of microscale scratching and wear and for nanoindentation hardness measurements and nanofabrication, a three-sided pyramidal single-crystal natural-diamond tip with a tip radius of about 100 nm is generally used [1] at relatively high loads ranging from 10 to 50 μ N.

2. Surface Roughness, Adhesion and Friction

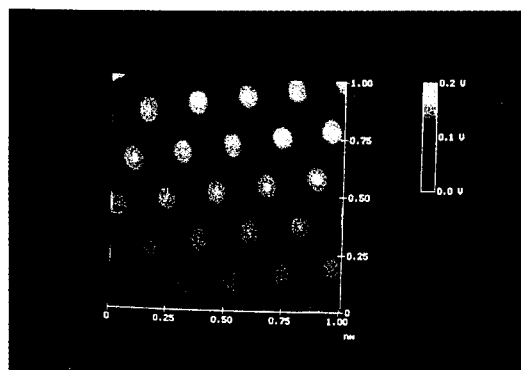
Solid surfaces, irrespective of the method of formation, contain surface irregularities or deviations from the prescribed geometrical form. When two nominally flat surfaces are placed in contact, surface roughness causes contact to occur at discrete contact points. Deformation occurs in these points, and may be either elastic or plastic depending on the nominal stress, surface roughness and material properties. The sum of the areas of all the contact points constitutes the real area that would be in contact, and for most materials at normal loads, this will be only a small fraction of the area of contact if the surfaces were perfectly smooth. In general, real area of contact must be minimized to minimize adhesion, fric-

tion and wear [3-4].

Characterizing surface roughness is therefore important for prediction and understanding the tribological properties of solids in contact. The AFM has been used to measure surface roughness on length scales from nanometers to micrometers. Surface roughness most commonly refers to the variations in the height of the surface relative to a reference plane [3,4,31-34]. Commonly measured roughness parameters, such as r.m.s. surface height and peak-to-valley distance, are found to be scale-dependent for any given surface. The topography of most engineering surfaces is fractal, possessing a self-similar structure over a range of scales. By using fractal analysis one can characterize roughness of surfaces with two scale-independent fractal parameters D and C which provide information about



Topography



Friction

Fig. 1(a). Grey-scale plots of surface topography (left) and friction profiles (right) of a 1×1 nm area of freshly cleaved HOPG, showing the atomic-scale variation of topography and friction.

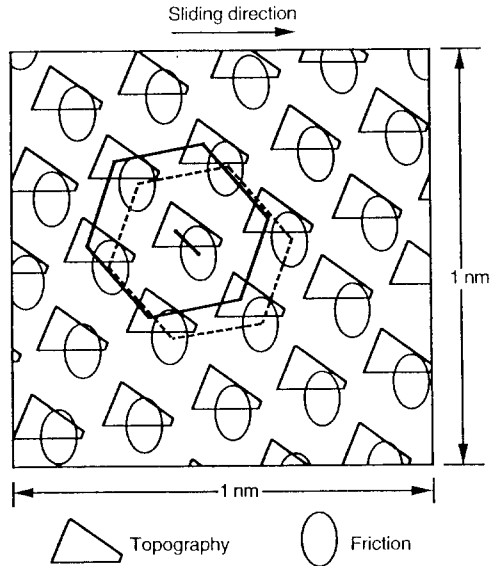


Fig. 1(b). Diagram of superimposed topography and friction profiles from (a); the symbols correspond to maxima. Note the spatial shift between the two profiles (Ref. 18).

roughness at all length scales [31-34]. These two parameters are instrument-independent and are unique for each surface. D (generally ranging from 1 to 2) primarily relates to distribution of different frequencies in the surface profile, and C to the amplitude of the surface height variations at all frequencies. A fractal model of elastic-plastic contact [23] has been used to predict whether contacts experience elastic or plastic deformation and to predict the statistical distribution of contact points.

To study friction mechanisms on an atomic scale, a well characterized freshly-cleaved surface of highly oriented pyrolytic graphite (HOPG) has been studied by Mate *et al* [11], and Ruan and Bhushan [18]. The atomic-scale friction force of HOPG exhibited the same periodicity same as that of corresponding topography (Fig. 1a), but the peaks in friction and those in topography were displaced relative to each other [18], (Fig. 1b). A Fourier expansion of the interatomic potential was used to calculate the conservative interatomic forces between atoms of the FFM tip and those of the graphite surface. Maxima in the interatomic forces in the normal and lateral directions do not occur at the same location, which explains the observed shift between the peaks in the lateral force and those in the corresponding to-

pography. Furthermore, the observed local variations in friction force were explained by variation in the intrinsic lateral force between the sample and the FFM tip [18] and these variations may not necessarily occur as a result of atomic-scale stick-slip process [11].

Friction forces of HOPG have also been studied [14,19,21,39]. Local variations in the microscale friction of cleaved graphite are observed, which arise from structural changes occur during the cleaving process [19]. The cleaved HOPG surface is largely atomically smooth but exhibits line-shaped regions in which coefficient of friction is more than order of magnitude larger. Transmission electron microscopy indicates that the line-shaped regions consist of graphite planes of different orientation, as well as of amorphous carbon. Differences in friction can also be seen for organic mon- and multi-layer films [14], which again seen to be the result of structural variations in the films. These measurements suggest that the FFM can be used for structural mapping of the surfaces. FFM measurements can be used to map chemical variations, as indicated by the use of the FFM with a modified probe tip to map the spatial arrangement of chemical functional groups in mixed organic monolayer films [39]. Here, sample regions that had stronger interactions with the functionalized probe tip exhibited larger friction. Local variations in the microscale friction of scratched surfaces can be significant, and seen to depend on the local surface slope rather than the surface height distribution [1, 15-21]. Directionality in friction is sometimes observed on the macroscale; on the microscale this is the norm [1,12,15-21]. This is because most 'engineering' surfaces have asymmetric surface asperities so that the interaction of the FFM tip with the surface is dependent on the direction of the asperities, which also causes asymmetry and directional dependence. Reduction in local variations and in directionality of frictional properties therefore requires careful optimization of surface roughness distributions and of surface-finishing processes.

Table 1 shows the coefficient of friction measured for two surface micro- and macroscales. The coefficient of friction is defined as the ratio of friction force to the normal load. The values on the microscale are much lower than those on the macroscale. When measured for the small contact areas

Table 1. Surface roughness and micro-and macro-scale coefficients of friction of various samples [17, 23,27]

| Material | R.M.S. roughness, nm | Micro-scale coefficient of friction versus Si ₃ N ₄ tip ¹ | Macro-scale coefficient of friction versus alumina ball ² |
|-----------------|----------------------|--|--|
| Si (111) | 0.11 | 0.03 | 0.18 |
| c+-implanted Si | 0.33 | 0.02 | 0.18 |

¹ Tip radius of about 50 nm in the load range of 10-150 nN (2.5-6.1 GPa), a scanning speed of 5 $\mu\text{m/s}$ and scan area of 1 $\mu\text{m} \times 1 \mu\text{m}$.

² Ball radius of 3 mm at a normal load of 0.1 N (0.3 GPa) and average sliding speed of 0.8 mm/s.

and very low loads used in microscale studies, indentation hardness and modulus of elasticity are higher than at the macroscale. This reduces the degree of wear. In addition, the small apparent areas of contact reduce the number of particles trapped at the interface, and thus minimize the 'ploughing' contribution to the friction force.

At higher load (with contact stresses exceeding the hardness of the softer material), however, the coefficient of friction for micro-scale measurements increases towards values comparable with those obtained from macroscale measurements, and surface damage also increases [23]. Thus Amontons' law of friction [3,4], which states that the coefficient of friction is independent of apparent contact area and normal load, does not hold for microscale measurements. These findings suggest microcomponents sliding under lightly loaded conditions should experience very low friction and near-zero wear.

3. Scratching, Wear and Indentation

The AFM can be used to investigate how surface materials can be moved or removed on micro-to nanoscales, for example in scratching and wear [15, 17,20,21,24] (where these things are undesirable), and nanomachining/nanofabrication (where they are desirable). The AFM can also be used for measurements of mechanical properties on micro-to nanoscales, Figure 2 show microscratches made on Si (111) at various loads after 10 cycles. As expected, the depth of scratch increases with load. Such microscratching measurements can be used to study failure mechanisms on the the microscale and

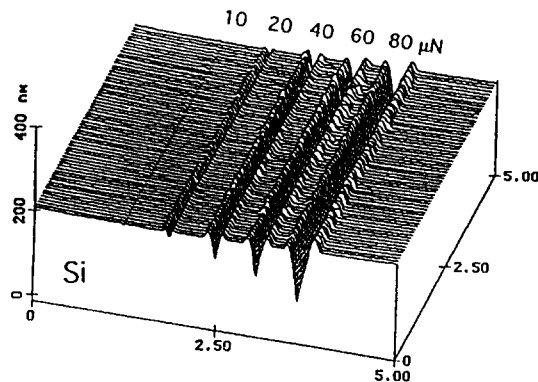


Fig. 2. Surface profiles of Si(111) scratched at various loads. Note that x and y axes are in μm and z axis is in nm (Ref. 17).

to evaluate the mechanical integrity (scratch resistance) of ultra-thin films at low loads [15,16].

By scanning the sample in two dimensions with the AFM, wear scars are generated on the surface. The evolution of wear of a diamond-like carbon coating on a polished aluminum substrate is shown in Fig. 3 which illustrates how the micro-wear profile for a load of 20 μN develops as a function of the number of scanning cycles¹⁶. Wear is not uniform, but is initiated at the nanoscratches indicating that surface defects (with high surface energy) act as initiation sites. Thus, scratch-free surfaces will be relatively resistant to wear.

Mechanical properties, such as hardness and modulus of elasticity can be determined on micro-to picoscales using AFM [16,17,20-22,35,-38]. Indentability on the scale of picometres can be studied by monitoring the slope of cantilever deflection as a function of sample traveling distance after the tip is engaged and the sample is pushed against the tip [15]. For a rigid sample, cantilever deflection equals the sample traveling distance; but the former quantity is smaller if the tip indents the sample. The indentation hardness of surface films with an indentation depth of as small as 1 nm has been measured for Si(111) [37] (Fig. 4). Triangular indentations are observed for shallow penetration depths. The hardness for and indentation depth of 2.5 nm is 16.6 GPa; and it drops to a value of 11.7 GPa at a depth of 7 nm. This decrease in hardness with increase in indentation depth can be rationalized on the basis that as the volume of deformed materials increase, there is a higher pro-

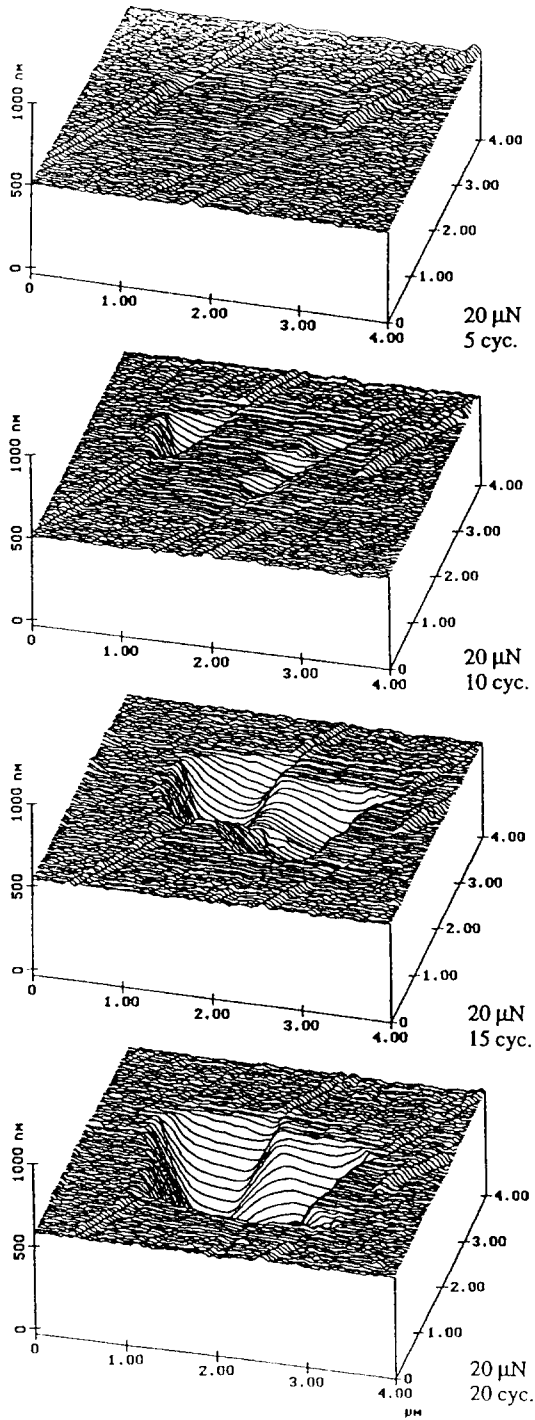


Fig. 3. Surface profiles of diamond-like carbon-coated thin-film disk showing the worn region; the normal load and number of test cycles are indicated (Ref. 16).

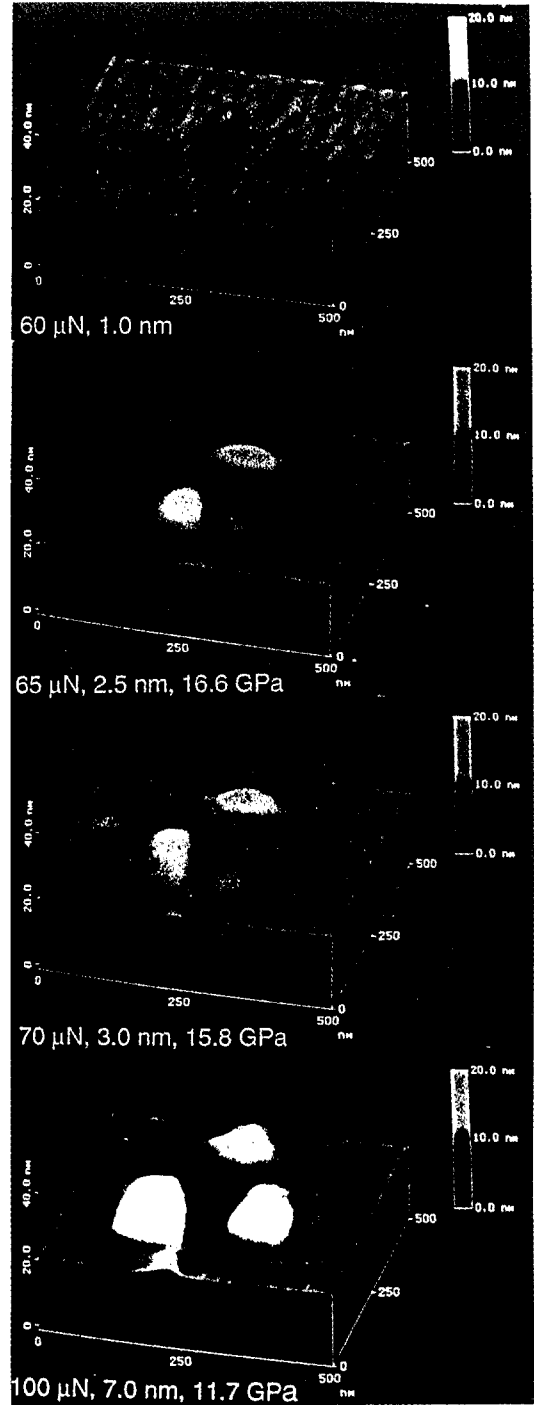
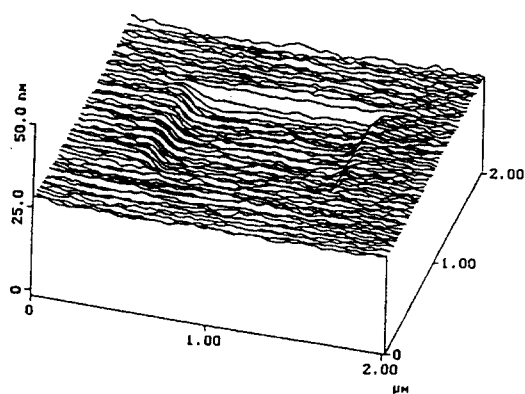


Fig. 4. Grey-scale plots of images of indentation marks on the Si(111) samples; load, indentation depths and hardness values are indicated (Ref. 37).

bability of encountering material defects [40]. Bhushan and Koinkar [17] have used AFM measurements to show that ion implantation of silicon surfaces increases their hardness and thus their wear resistance. Formation of surface alloy films with improved mechanical properties by ion implantation is growing technological importance as means of improving the mechanical properties of materials.

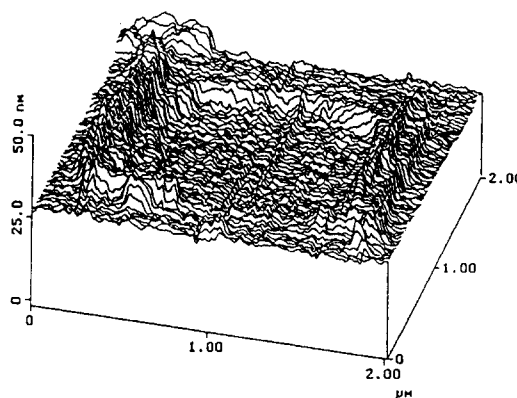
The Young's modulus of elasticity is calculated from the slope of the indentation curve during unloading [1,35,38]. Maivald *et al* [36], used an AFM in 'force mode' to measure surface elasticities: AFM tip is scanned over the modulated sample surface with the feedback loop keeping the average force constant. For the same applied force, a soft area deforms more, and thus causes less cantilever deflection, than a hard area. The ratio of modulation amplitude to the local tip deflection is then used to create a 'force modulation image'. The force modulation mode makes in easres on hard substrates.

Detection of transfer of material on a nanoscale is possible with the AFM. Indentation C_{60} -rich fullerene films with an AFM tip has been shown [41] to result in the transfer of fullerene molecules to the AFM tip, as indicated by discontinuities in the cantilever deflection as a function of sample traveling distance in subsequent indentation studies.



C_{18} double grafted/ SiO_2 / Si

40 μN , 3.7 nm



$ZnA/ODT/Au/Si$

200 nN, 6.5 nm

Fig. 6. Surface profiles showing the worn region after one scan cycle for self-assembled monolayers of octadecyl silanol (C_{18}) (left) and zinc arachidate (ZnA) (right). Normal force and wear depths are indicated. Note that wear of ZnA occurs at only 200 nN as compared to 40 μN for C_{18} film (Ref. 27).

4. Boundary Lubrication

The 'classical' approach to lubrication uses freely supported multimolecular layers of liquid lubricant [1,6,25,26,28-30]. The liquid lubricants are chemically bonded to improve their wear resistance [3]. To study depletion of boundary layers, the micro-scale friction measurements were made as function of number of cycles virgin $Si(100)$ surface and silicon surface lubricated with about 2-nm thick Z-15 and Z-Dol PEPE lubricants, Fig. 5 Z-Dol is PFPE lubricant with hydroxyl end groups. Its lubricant film

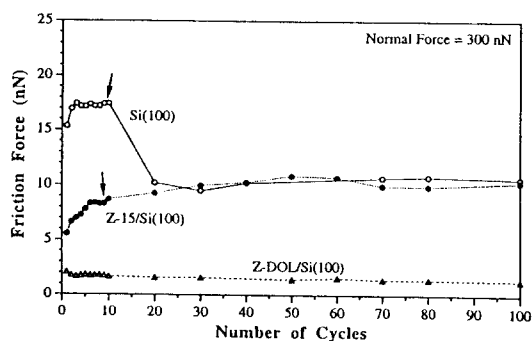


Fig. 5. Friction force as a function of number of cycles using silicon nitride tip at a normal force of 300 nN for the unlubricated and lubricated silicon samples (Ref. 29).

was thermally bonded at 150°C for 30 minutes and washed off with a solvent to provide a chemically bonded layer to the lubricant film. In Fig. 5, the unlubricated silicon sample shows a slight increase in friction force followed by a drop to a lower steady state value after 20 cycles. Depletion of native oxide and possible roughening of the silicon sample are believed to be responsible for the decrease in friction force after 20 cycles. The initial friction force for Z-15 lubricated sample is lower than that of unlubricated silicon and increase gradually to friction force value comparable to that of the silicon after 20 cycles. This suggests the depletion of the Z-15 lubricant in the wear track. In the case of the Z-Dol coated silicon sample, the friction force starts out to be low and remains low during the 100 cycles test. It suggests that Z-Dol does not get displaced/depleted as readily as Z-15. Additional studies of freely supported liquid lubricants showed that either increasing the film thickness or chemically bonding the molecules to the substrate with a mobile fraction improves the lubrication performance [28,29,30].

For lubrication of microdevices, a more effective approach involves the deposition of organized, dense molecular layers of long-chain molecules on the surface contact. Such monolayers and thin films are commonly produced by Langmuir-Blodgett (L-B) deposition and by chemical grafting of molecules into self-assembled monolayers (SAMs). Based on the measurements, SAMs of octadecyl (C_{18}) compounds based on aminosilanes on an oxidized silicon exhibited lower coefficient of friction (0.018) and greater durability than LB films of zinc arachidate adsorbed on a gold surface coated with octadecylthiol (ODT) (coefficient of friction of 0.03) (Fig. 6) [27]. LB films are bonded to the substrate by weak van der Waals attraction, whereas, SAMs are chemically bound via covalent bonds. Because of the choice of chain length and terminal linking group that SAMs offer, they hold great promise for boundary lubrication of microdevices.

Measurement of ultra-thin lubricant films with nanometer lateral resolution can be made with the AFM [42-44]. The lubricant thickness is obtained by measuring the force on the tip as it approaches, contacts and pushes through the liquid film and ultimately contacts the substrate. The distance between the sharp 'snap-in' (owing to the formation of a liquid meniscus between the film and the tip)

at the liquid surface and the hard repulsion at the substrate surface is a measure of the liquid film thickness. This technique is now used routinely in the information-storage industry for thickness measurements (with nanoscale spatial resolution) of lubricant films, a few nanometres thick, in rigid magnetic disks.

References

1. Bhushan, B., Handbook of Micro/Nanotribology (CRC, Boca Raton, Florida), 1995.
2. Bhushan, B., Israelachvili, J.N. and Landman, U., Nature 374, 607-616, 1995. (Clarendon, Oxford, 1950 & 1964).
4. Bhushan, B., Tribology and Mechanics of Magnetic Storage Devices, Springer, New York, 1990.
5. Bhushan, B. and Gupta, B. K. Handbook of Tribology: Materials, Coatings and Surface Treatments, McGraw-Hill, New York, 1991.
6. Blackman, G.S., Mate, C.M. and Phipps, M.R. Phys. Rev. Lett. 65, 2270-2273, 1990.
7. Burnham, N.A., Domiguez, D.D., Mowery, R.L. and Colton, R.J. Phys. Rev. Lett. 64, 1931-1934, 1990.
8. Landman, U., Luedtke, W.D., Brunham, N.A. and Colton, R.J., Science 248, 454-461, 1990.
9. Ducker, W.A., Senden, T.J. and Pashley, R.M. Langmuir 8, 1831-1836, 1992.
10. Salmeron, M., Neubauer, G., Folch, A., Tomitori, M., Ogletree, D.F., and Sautet, P. Langmuir 9, 3600-3611, 1993.
11. Mate, C.M., McClelland, G.M., Erlandsson, R. and Chiang, S. Phys. Rev. Lett. 59, 1942-1945, 1987.
12. Meyer, G. and Amer N.M. Apple. Phys. Lett., 57, 2089-2091, 1990.
13. Kaneko, R., Miyamoto, T. and Hamada, E., Adv. Info. Storage Syst. 1, 267-277, 1991.
14. Meyer, E., Overmyer, R., Luthi, R., Brodbeck, D., Howald, L., Formmer, J., Guntherodt, H.J., Wolter, O., Fujihira, M. Takano, T., and Gotoh, Y., Thin Solid Films 220, 132-137, 1992.
15. Bhushan, B. and Ruan, J., ASME J. Tribology, 116, 389-396, 1994.
16. Bhushan, B., Koinkar, V.N. and Ruan, J. Proc Instn. Mech. Engrs. Part J: J. Eng. Tribol. 208, 17-29, 1994.
17. Bhushan, B. and Koinkar, V.N. J., Appl. Phys. 75, 5741-5746, 1994.

18. Ruan, J. and Bhushan, B.J., *Appl. Phys.* 76, 5022-5035, 1994.
19. Ruan, J. and Bhushan, B.J., *Appl. Phys.* 76, 8117-8120, 1994.
20. Bhushan, B. and Koinkar, V.N., *Tribology Trans.* 38, 119-127, 1995.
21. Bhushan, B. and Koinkar, V.N., *Wear* 180, 9-6, 1995; 183, 360-370, 1995.
22. Koinkar, V.N. and Bhushan, B., *Surface Coatings and Technol.* (in press).
23. Bhushan, B. and Kulkarni, A.V., *Thin Solid Films* (in press).
24. Miyamoto, T., Kaneko, R. and Miyake, S.J., *Vac. Sci. Technol.* B9, 1336-1339, 1991.
25. Mate, C.M., *Phys. Rev. Lett.* 68, 3323-3326, 1992.
26. O'Shea, S.J., Welland, M.E. and Rayment, T., *Appl. Phys. Lett.* 61, 2240-2242, 1992.
27. Bhushan, B., Kulkarni, A.V., Koinkar, V.N., Boehm, M., Odoni, L., Martelet, C., and Belin, M., *Langmuir* 11, 3189-3198.
28. Bhushan, B., Miyamoto, T. and Koinkar, V.N., *Adv. Info. Storage Syst.* 6, 151-161, 1995.
29. Koinkar, V.N. and Bhushan, B., *J. Vac. Sci. Technol.* (in press).
30. Koinkar, V.N. and Bhushan, B., *J. Appl. Phys.* (in press).
31. Majumdar, A. and Bhushan, B., *ASME J. Tribology* 112, 205-216, 1990.
32. Majumdar, A. and Bhushan, B., *ASME Journal of Tribology* 113, 1-11, 1991.
33. Bhushan, B. and Majumdar, A., *Wear* 153, 53-64, 1992.
34. Ganti, S. and Bhushan, B., *Wear* 180, 17-34, 1995.
35. Burnham, N.A. and Colton, R.J., *J. Vac. Sci. Technol.* A7, 2906-2913, 1989.
36. Maivald, P., Butt, H.J., Gould, S.A.C., Prater, C.B., Drake, B., Gurley, J.A., Elings, V.B., and Hansma, P.K., *Nanotechnology* 2, 103-106, 1991.
37. Bhushan, B. and Koinkar, V.N., *Appl. Phys. Lett.*, 64, 1653-1655, 1994.
38. Bhushan, B., Kulkarni, A.V., Bonin, W. and Wyrobek, J., *Phil. Mag.* (submitted).
39. Frisbie, C.D., Rozsnyai, L.F., Noy, A., Wrighton, M.S. and Lieber, C.M., *Science* 265, 2071-2074.
40. Gane, N. and Cox, J.M., *Phil. Mag.* 22, 881-891, 1970.
41. Ruan, J. and Bhushan, B.J. *Mater. Res.* 8, 3019-3022, 1993.
42. Mate, C.M., Lorenz, M.R. and Novotny, V.J., *J. Chem. Phys.* 90, 7550-7555, 1989.
43. Blackman, G.S., Mate, C.M. and Philpott, M.R. *Phys. Rev. Lett.* 65, 2270-2273, 1990.
44. Bhushan, B. and Blackman, G.S., *ASME J. Tribol.* 113, 452-458, 1991.